Theory of Surface Deformations of Polymer Brushes in Solution

A. E. Likhtman,[†,‡,§,||] S. H. Anastasiadis,[‡] and A. N. Semenov*,[†,‡,§,||]

Physics Department, Moscow State University, Moscow 117234, Russia; Institute of Electronic Structure and Laser, Foundation for Research and Technology—Hellas, P.O. Box 1527, 71110 Heraklion, Crete, Greece; Physics Department, University of Crete, 710 03 Heraklion, Crete, Greece; and Department of Applied Mathematical Studies, University of Leeds, Leeds LS2 9JT, U.K.

Received April 13, 1998; Revised Manuscript Received February 23, 1999

ABSTRACT: The excess free energy of small-amplitude deformations of a wet "parabolic" brush consisting of polymer chains attached to a solid plane by one end is calculated. The brush is swollen by a good (marginal) solvent. A generic deformation involving both compression normal to the grafting surface and lateral shear is considered. It is shown that the free energy attains a minimum as a function of the wave vector of the deformation, $\mathbf{q}$. A shallow maximum of the scattering function $S(\mathbf{q})$ is thus predicted. The theoretical scattering functions calculated for an arbitrary orientation of the scattering vector are compared with evanescent-wave light scattering data.

1. Introduction

Polymer chains attached by one end to a plane solid surface or a liquid−liquid interface at sufficiently high surface coverage are known as polymer brushes.[1,2] Understanding of the equilibrium and nonequilibrium properties of brushes is useful with regard to fine-tuning surface properties of materials using grafted polymer layers.

The aim of the present paper is to study theoretically the deformation behavior of "wet" polymer brushes swollen in a marginal solvent. The surface waves we consider can be probed, for example, by evanescent-wave light scattering.

The first theoretical investigation of brush deformations was performed by Fredrickson et al.[3] for the case of a molten polymer brush (i.e., without solvent). They used the Alexander brush approximation[4] and assumed that all free chain ends lie at the free brush surface. Using this approximation, they found that the deformation free energy per unit area of grafting surface for a small-amplitude sinusoidal deformation with wave vector q and amplitude ϵ can be written as

$$f_t = f^{(0)} + \gamma\,(1 + \epsilon^2 q^2/4) + \frac{1}{4}\left(\frac{\epsilon}{h_0}\right)^2 \mu_0 h_0 \{3(qh_0)^{-2} + 2qh_0\} + \mathrm{O}(\epsilon^4) \quad (1)$$

where $f^{(0)} = 3v^2\sigma^3 N/2b^2$ is the free energy of the undeformed melt polymer brush in the Alexander approximation, γ is the surface tension of the polymer−air interface, $\mu_0 = 3k_BTv\sigma^2/b^2$ is the shear modulus of the brush, and h_0 is the equilibrium brush height. The second term in eq 1 describes the surface tension contribution, and the third term accounts for the stretching entropy in the limiting cases of low and high q's; N is the number of segments per grafted chain, b is the statistical segment length, and σ is the brush surface density (number of attached chains per unit area). The segmental volume v is used as a volume unit and k_BT as the energy unit. In the following, the notation $a = b/\sqrt{6}$ is used.

A later analysis of Xi and Milner[5] showed that the term $(2qh_0)$ in eq 1 is an artifact of the Alexander approximation. Xi and Milner[5] allowed for an arbitrary distribution of free ends inside the brush. They also allowed the chain trajectories to be curved: they introduced an additional function which describes deviations of polymer chain trajectories from straight lines. It was also assumed[5] that the chain paths do not intersect each other; this assumption is not used in the present paper (see section 2.2). For the stretching deformation energy of the molten brush (without the surface tension contribution), Xi and Milner obtained

$$\frac{F}{F_0} = 1 + \epsilon^2\left(\frac{3}{2} + \frac{1.675}{(qh_0)^2}\right) \quad (2)$$

which differs slightly from eq 1 in the limit of small q's (a coefficient of 1.675 instead of 1.5). Here F_0 is the undeformed free energy per unit area of the parabolic molten brush; $F_0 = \pi^2 N\sigma^3 v^2/(8b^2)$, which is smaller by a factor $12/\pi^2$ than that of the "step-function brush".

The theory of brush deformations is generalized in the present paper along the following lines: (i) all assumptions about the chain trajectories are lifted, (ii) we allow for an arbitrary orientation of the deformation wave vector, and (iii) the effect of good solvent is considered. In the next section, we calculate the excess free energy for a small sinusoidal brush deformation. The correlation function of the concentration fluctuations is calculated as well. We consider simultaneous shear deformation modes (displacements parallel to the layer) and breathing modes (normal displacements) in the general case, i.e., for an arbitrary orientation of the scattering wave vector. The predictions are then compared with experimental results in section 3.

2. Free Energy Calculations

2.1. Equilibrium Brush. The free energy of an equilibrium brush consists of two main terms:[2] the chain stretching energy F_{el} and the osmotic energy F_{osm} due to excluded-volume interactions of monomers

---

[†] Moscow State University.

[‡] Foundation for Research and Technology—Hellas.

[§] University of Crete.

[||] University of Leeds.

10.1021/ma980572s CCC: $18.00

$$F = F_{\mathrm{el}} + F_{\mathrm{osm}} = \sum_{\text{all chains}} \int_0^N \mathrm{d}n \left[\frac{1}{4a^2}\left(\frac{\mathrm{d}\mathbf{r}_n}{\mathrm{d}n}\right)^2\right] + \frac{1}{2}w \int \mathrm{d}^3 r \phi_0^2(r) \quad (3)$$

where $\mathbf{r}_n$ is the position of the nth monomer ($n = 0$ corresponds to the beginning of the chain at the solid wall and $n = N$ to its end), $\phi_0(\mathbf{r})$ is the equilibrium monomer density, and w is the monomer interaction parameter which is equal to the monomer excluded volume in the athermal case.

The elastic free energy given by the first term on the right-hand side (rhs) of eq 3 is valid for strongly stretched brushes when the elastic energy per grafted chain is much larger than k_BT. The second term in the rhs represents a mean-field approximation for the osmotic free energy, which is accurate if the solvent is marginal, i.e. if $w/(b^6\phi_0) < 1$, where ϕ_0 is the characteristic monomer concentration (see Grosberg and Khokhlov[6]). The mean-field approximation implies that each monomer is influenced by an average molecular potential U which is proportional to the local monomer concentration. It has been shown[2,7] that the effective molecular field, $U(\mathbf{r})$, inside the brush must have a simple quadratic form

$$U_0(z) = A_0 - Bz^2 \quad (4)$$

where z is the height (the distance from the grafting surface),

$$B = \frac{\pi^2}{16N^2a^2} \quad (5)$$

and A_0 is determined by the boundary conditions; the subscript zero is used to denote an equilibrium value. The parabolic field is the only self-consistent solution; a different field can not be consistent with the fact that the free ends are distributed inside the brush. The parabolic molecular field is valid for a polymer brush in both the melt and the solution. In the solution case, the molecular potential is related to the monomer density, $U(\mathbf{r}) = w\phi_0(\mathbf{r})$. The monomer concentration at the brush edge must vanish: $\phi(h_0) = U(h_0)/w = 0$, so we have $A_0 = Bh_0^2$. Minimizing the total free energy F (eq 3) with respect to the brush height, h_0, we obtain:

$$A_0 = \frac{1}{4}\left(\frac{3\pi\sigma w}{a}\right)^{2/3}; \quad F_0 = \frac{9}{10}\left(\frac{\pi^2}{24}\right)^{1/3} N\sigma\left(\frac{\sigma w}{a}\right)^{2/3}; \quad h_0 = \left(\frac{24}{\pi^2}\right)^{1/3} N(\sigma w a^2)^{1/3} \quad (6)$$

where F_0 is the equilibrium brush free energy *per unit area*.

2.2. Deformed Brush: Elastic Free Energy. To calculate the free energy of a deformed brush, we first consider the brush in a small external potential $\epsilon(\mathbf{r})$ which we define as potential energy of a monomer at position $\mathbf{r}$. For simplicity, we assume that the field is uniform along the y-axis (the x-axis is parallel and the z-axis is perpendicular to the grafting surface). Thus, the problem is essentially two-dimensional. The total field is then the sum of the external field $\epsilon(\mathbf{r})$ and the molecular field $u_{\mathrm{mol}} = w\phi(\mathbf{r})$. The total field $U_{\mathrm{tot}} = w\phi + \epsilon$ should be parabolic as in the case of the equilibrium brush (eq 4) for the same reason: $U_{\mathrm{tot}} = A(x) - Bz^2$ where $A(z)$ is an arbitrary function slightly different from A_0. A small field produces a small density variation; hence, we can represent the total density as a sum of the equilibrium density $\phi_0(z) = 1/w(A_0 - Bz^2)$ (see the previous section) plus a small increment: $\phi(\mathbf{r}) = \phi_0(z) + \delta\phi(\mathbf{r})$. Thus, the total field variation $u(\mathbf{r}) \equiv U_{\mathrm{tot}}(\mathbf{r}) - U_0(\mathbf{r})$ does not depend on z:

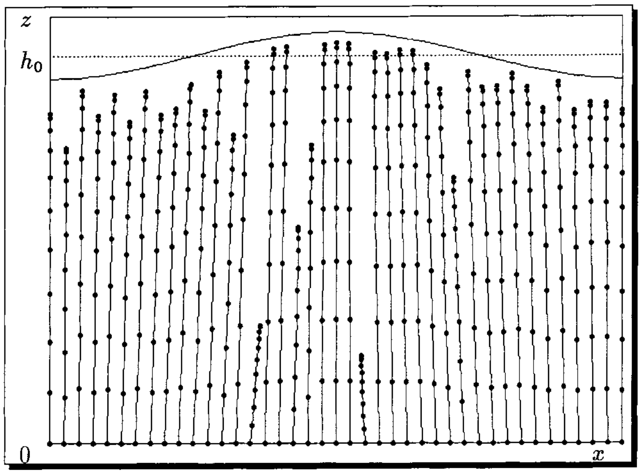

Figure 1. Schematic picture of a deformed polymer brush. The lines show the chain trajectories, and the density of dots on each line shows the degree of chain stretching, e.g., low density means high stretching. Note that for simplicity not all polymer chains are shown but only those with free ends near the free surface (brush edge) and near the midplane (halfway from the grafting plane to the brush edge).

$$u(\mathbf{r}) = \epsilon(\mathbf{r}) + w\delta\phi(\mathbf{r}) = A(x) - A_0 = u(x) \quad (7)$$

The remaining problem is to calculate the single-chain response to the perturbation field $u(x)$. The force balance equation for the nth monomer is

$$\frac{1}{2a^2}(\mathbf{r}_{n-1} - 2\mathbf{r}_n + \mathbf{r}_{n+1}) - \nabla[w\phi_0(z) + u(x)] = 0$$

or in the continuous limit for the x-projection,

$$\frac{1}{2a^2}\frac{\partial^2 x(n)}{\partial n^2} = \frac{\partial u(x)}{\partial x}; \quad x(0) = x_0; \quad \frac{\partial x}{\partial n}\Big|_{n=N} = 0$$

The boundary conditions imply that the first chain monomer is attached to the solid at point $(0, x_0)$ and the last (Nth) monomer is free so that the chain tension must vanish there (see Figure 1).

The solution of this equation for a small field $u(x)$ is $x = x_0 + \Delta(x, n) = x_0 + a^2(\partial u/\partial x)[(n - N)^2 - N^2]$, where $\Delta(x, n)$ is the displacement of the nth monomer with coordinate x in the x-direction and the derivative $\partial u/\partial x$ must be calculated at $z = x_0$. To calculate the integral density change $\delta\Phi(x) = \int_0^h \phi(x, z)\, \mathrm{d}z$, we first consider the equilibrium density of monomers with number n, $\Phi_0(n)$, which is obviously equal to the grafting density $\Phi_0(n) = \sigma$. Thus the continuity equation for these monomers is

$$\delta\Phi(x, n) = -\frac{\partial\Delta(x, n)}{\partial x}\sigma = a^2u''(x)\sigma[N^2 - (n - N)^2] \quad (8)$$

where $\delta\Phi(x, n)$ is the density change due to displacement of the nth monomers and $u''(x)$ means the second derivative along the x-direction. To determine the total density change $\delta\Phi(x)$, we integrate eq 8 over n and substitute eq 6 for h_0:

$$\delta\Phi(x) = \int_0^N \delta\Phi(x, n)\, \mathrm{d}n = \frac{\pi^2}{36}\frac{u''(x)}{w}h_0^3$$

On the other hand, eq 7 implies that

$$\int_0^{h_0} \delta\phi(x, z)\, \mathrm{d}z = \frac{h_0}{w}[u(x) - E(x)]$$

where $E(x) = (1/h_0)\int_0^{h_0} \epsilon(x, z)\, \mathrm{d}z$ is the external field averaged over z. Thus, we arrive at the following equation for the total field change:

$$-\frac{\pi^2}{36}h_0^2 u''(x) + u(x) = E(x)$$

In the case of a harmonic external field $\epsilon(\mathbf{r}) = \epsilon e^{i\mathbf{qr}}$, where ϵ is a small amplitude, we get $E(x) = i\epsilon e^{iq_x x}/h_0 q_z)$-$(1 - e^{iq_z h_0})$. Thus,

$$u(x) = \frac{i\epsilon(1 - e^{iq_z h_0})}{h_0 q_z\left(1 + \frac{\pi^2}{36}q_x^2 h_0^2\right)} e^{iq_x x}$$

and the density fluctuation

$$\delta\phi(\mathbf{r}) = \frac{1}{w}[u(x) - \epsilon(\mathbf{r})] = \frac{\epsilon}{w}\left[\frac{i(1 - e^{iq_z h_0})}{h_0 q_z\left(1 + \frac{\pi^2}{36}q_x^2 h_0^2\right)} e^{iq_x x} - e^{i\mathbf{qr}}\right] \quad (9)$$

To calculate the average density fluctuation in a brush (without external field), we use the fluctuation–dissipation theorem,[8] which relates the density fluctuations to the susceptibility:

$$\langle \delta\phi(\mathbf{q})\delta\phi(-\mathbf{q})\rangle = T\chi_c(\mathbf{q}, \mathbf{q})$$

where the susceptibility $\chi_c(\mathbf{k}, \mathbf{k}')$ is the proportionality coefficient between the density variation and the conjugate external field:[9]

$$\delta\phi(\mathbf{k}) = -\int \chi_c(\mathbf{k}, \mathbf{k}')\epsilon(\mathbf{k}')\frac{\mathrm{d}\mathbf{k}'}{(2\pi)^2} \quad (10)$$

Equation 10 can be transformed using

$$\epsilon(\mathbf{k}') = \epsilon\int e^{i\mathbf{r}(\mathbf{q}-\mathbf{k}')}\, \mathrm{d}\mathbf{r} = \epsilon(2\pi)^2\delta(\mathbf{q} - \mathbf{k}')$$

to the simple relation (for $\mathbf{k} = \mathbf{q}$)

$$\delta\phi(\mathbf{q}) = -\epsilon\chi_c(\mathbf{q}, \mathbf{q})$$

so that $\chi_c(\mathbf{q}, \mathbf{q}) = -\delta\phi(\mathbf{q})/\epsilon$. Taking the Fourier transformation of eq 9, we get

$$\delta\phi(\mathbf{q}) = -\frac{Lh_0\epsilon}{w}f_c(h_0\mathbf{q});$$

$$\text{where } f_c(h_0\mathbf{q}) = 1 - \frac{4\sin^2(h_0\mathbf{q}_z/2)}{h_0^2 q_z^2\left(1 + \frac{\pi^2}{36}q_x^2 h_0^2\right)}$$

and L is the brush size in the x-direction. So, the susceptibility is

$$\chi_c(\mathbf{q}, \mathbf{q}) = \frac{Lh_0}{w}f_c(h_0\mathbf{q})$$

The real external field $\epsilon'(\mathbf{r}) = R(\epsilon e^{i\mathbf{qr}}) = \epsilon\cos\mathbf{qr}$ produces a density fluctuation

$$\delta\phi'(\mathbf{r}) = \frac{\epsilon}{w}\left[\frac{2\sin(h_0 q_z/2)}{h_0 q_z\left(1 + \frac{\pi^2}{36}q_x^2 h_0^2\right)}\cos(xq_x + h_0 q_z/2) - \cos\mathbf{qr}\right] \quad (11)$$

The elastic free energy (due to chain stretching) is minus one half of the energy in the external field:

$$\Delta F_c = -\frac{1}{2}\int \epsilon'(\mathbf{r})\delta\phi'(\mathbf{r})\, \mathrm{d}x\, \mathrm{d}z = \frac{\epsilon^2 L h_0}{4w}f_c(h_0\mathbf{q}) \quad (12)$$

2.3. Gradient Term. We should take into account another contribution to the deformation free energy of the brush in a good solvent related to its surface distortion: The monomer density of the deformed brush is strongly inhomogeneous near the edge where the density itself tends to zero, and the relative gradient $\nabla\phi/\phi$ is high in this region, giving rise to an additional entropic contribution to the free energy. This contribution is approximately given by the standard square-gradient term, F_{gr}, accounting well for short-scale inhomogeneities:

$$F = F_{el} + F_{osm} + F_{gr}$$

where $F_{el} + F_{osm}$ stands for the rhs of eq 3. The gradient free energy is[9,10]

$$F_{gr} = \frac{a^2}{4}\int_0^L \mathrm{d}x \int_0^{h(x)} \mathrm{d}z \frac{(\nabla\phi(x, z))^2}{\phi(x, z)} \quad (13)$$

Here, $h(x)$ is the "local" brush height above point x on the grafting plane; the monomer density, eq 11, tends to zero at $z = h(x)$. Note that the local degree of chain stretching is also small near the free surface $z = h(x)$. However, the monomer density gradient $\nabla\phi$ attains its maximum in this region in the deformed brush. Therefore, the gradient free energy is dominant in the region near the free surface.

Equation 13 and the density profile eq 11 formally produce a logarithmic singularity near the free surface where the density tends to zero. Note however that eq 11 can be applied only in the "classical" region where the chains are strongly stretched. Hence, this equation is valid in the region $0 < z < h - \xi$, where ξ is the thickness of the so-called interpenetration layer.[11] It can be estimated using this condition that the chain terminal fragments are not stretched in the interpenetration region, and so, their Gaussian size is $\xi \sim ag^{1/2}$, where g

$\sim N\sqrt{\xi/R}$ is the number of monomers in the layer of thickness ξ. Thus $\xi \sim N^{2/3}a^{4/3}h_0^{-1/3}$.

Hence, the monomer concentration profile is smeared out in the ξ-layer near the classical free surface, leading to an effective cut-off of the logarithmic singularity in eq 13 at $z \simeq h - \xi$; i.e., the upper limit limit in the integral over z in eq 13 must be changed to $h(x) - \xi$. The function $h(x)$ can be found from the condition $\phi[x, h(x)] = 0$; i.e., $\phi_0[h(x)] + \delta\phi[x, h(x)] = (B/w)[h_0^2 - h^2(x)] + \delta\phi[x, h(x)] = 0$. The solution to the last equation can be represented as a series expansion:

$$h(x) \approx h_0 + \frac{w\delta\phi(x, h_0)}{2Bh_0} - \frac{w^2\delta\phi^2(x, h_0)}{8B^2h_0^3} + \frac{w^2\delta\phi(x, h_0)\dfrac{\partial\delta\phi}{\partial z}}{4B^2h_0^2} + O(\delta\phi^3)$$

Let us assume that

$$\delta\phi_{\text{tot}} = \alpha\delta\phi \tag{14}$$

where $\delta\phi_{\text{tot}}$ is the density deviation induced by the external field $\epsilon(\mathbf{r})$, including the gradient term effect, and $\delta\phi$ is the induced density fluctuation calculated in the previous section (i.e., neglecting the gradient energy); α is a coefficient. The total susceptibility is thus proportional to the susceptibility without the gradient energy:

$$\chi(\mathbf{q}, \mathbf{q}) = \alpha\chi_c(\mathbf{q}, \mathbf{q}) \tag{15}$$

To determine α, let us calculate the gradient free energy for the density fluctuation defined in eq 11:

$$\begin{gathered} F_{\text{gr}} = \frac{\pi^2}{32}\frac{1}{N^2}\frac{Lh_0}{w}\ln\left(\frac{h_0}{\xi}\right) + \Delta F_{\text{gr}}; \\ \Delta F_{\text{gr}} = \frac{\epsilon^2}{32}\frac{\pi^{2/3}}{3^{4/3}}\frac{1}{N^2}\frac{Lh_0}{w}\ln\left(\frac{h_0}{\xi}\right)\left(\frac{a}{\sigma w}\right)^{4/3} f_{\text{gr}}(h_0\mathbf{q}); \\ f_{\text{gr}}(h_0\mathbf{q}) = 14h_0^2q_z^2 - 1 + 2h_0^2q_x^2 + (-1 + 2h_0^2q_x^2) \left[\frac{2\sin(h_0q_z/2)}{h_0q_z\left(1 + \frac{\pi^2}{36}q_x^2h_0^2\right)}\right]^2 + [\cos(q_zh_0/2)(-4q_x^2h_0^2 + 2 - \\ 6q_z^2h_0^2) + 2q_zh_0\sin(q_zh_0/2)]\left[\frac{2\sin(h_0q_z/2)}{h_0q_z\left(1 + \frac{\pi^2}{36}q_x^2h_0^2\right)}\right] \end{gathered} \tag{16}$$

The total free energy change, ΔF, associated with the induced density fluctuation $\delta\phi_{\text{tot}}$ can be calculated using two different approaches. On the one hand, using eqs 12 and 14, we get

$$\Delta F = \frac{1}{2}\int \chi^{-1}(k, k')\delta\phi_{\text{tot}}(k)\delta\phi_{\text{tot}}(k')\,\mathrm{d}k\,\mathrm{d}k' = \alpha\Delta F_c \tag{17}$$

On the other hand, ΔF is the sum of the gradient and the conformation/osmotic free energy increments due to the total density fluctuation $\delta\phi_{\text{tot}} = \alpha\delta\phi$. Because ΔF is a quadratic form in $\delta\phi$, we get

$$\Delta F \equiv \Delta F[\delta\phi_{\text{tot}}] = \alpha^2\Delta F[\delta\phi] = \alpha^2(\Delta F_c + \Delta F_{\text{gr}}) \tag{18}$$

where ΔF_c and ΔF_{gr} are defined in eqs 12 and 16. Thus using eqs 15, 17, and 18 we obtain

$$\alpha = \frac{\Delta F_c}{\Delta F_c + \Delta F_{\text{gr}}};\quad \chi(\mathbf{q}, \mathbf{q}) = \frac{Lh_0}{w}\frac{f_c^2(h_0\mathbf{q})}{f_c(h_0\mathbf{q}) + \beta f_{\text{gr}}(h_0\mathbf{q})} \tag{19}$$

where

$$\beta = \frac{\pi^{2/3}}{8 \times 3^{4/3}}\frac{1}{N^2}\left(\frac{a}{\sigma w}\right)^{4/3}\ln\left(\frac{h_0}{\xi}\right)$$

3. Comparison with Experiment

The thermal fluctuations of the segment density profile of a polymer brush formed by end-attached polystyrene chains exposed to a good solvent have been recently probed by dynamic light scattering in an evanescent wave configuration.[16] The polymer sample was asymmetric poly(ethylene oxide-*b*-styrene) (PEO−PS) copolymer, with the short PEO blocks strongly adsorbed by the glass prism.

In this setup, the evanescent light wave, produced under total reflection conditions, was utilized as an incident beam in the scattering experiment, and the time correlation functions $C(q, t)$ of the concentration fluctuations with wave vector $\mathbf{q}$ were measured using photon correlation spectroscopy. A set of terminally attached layers with thickness (h_0) varied from 45 to 130 nm were studied. It was found that the static scattering intensity attains a maximum at $q \sim O(h_0^{-1})$. The penetration depth of the evanescent wave was much larger than the brush height, indicating that fluctuations of the integrated concentration over the brush height were probed.

Below, we consider the scattering function $S(\mathbf{q})$, which was measured directly in the experiments[16] and which is related to the density fluctuations: $S(\mathbf{q}) = \chi(\mathbf{q}, \mathbf{q})$. Thus with eq 19, we predict $S(\mathbf{q})$ as a function of the two components of the scattering vector, q_x and q_z, and one additional dimensionless parameter β, which governs the contribution of the gradient term ($\beta = 0$ means that this term is neglected). The 3-D plot of $S(\mathbf{q})$ for different β is shown in Figure 2. The scattering intensity decreases as the β parameter is increased because the gradient free energy tends to suppress fluctuations. It is clear from the figure that the effect is significant for large q, i.e. for short wavelength fluctuations. However for experimental values $qh_0 < 5$ and $\beta < 10^{-4}$, the effect of the gradient term is almost negligible. The position of the maximum intensity shifts to lower q_x as β is increased.

In the evanescent-wave experiment,[16] the scattering measurements were carried out for a particular trajectory in the q-space:

$$q_x = k(1 - \cos\theta);\quad q_z = k\sin\theta \tag{20}$$

where θ is the scattering angle and k is the wave vector of the evanescent wave utilized as the incident beam in the scattering experiment. The scattering function $S(\theta)$ is determined by the intersection of the surface $S(\mathbf{q})$ and the cylinder, eq 20, which is depicted in Figure 3 for different kh_0. Note that the maximum here is determined not by the gradient term but rather by the particular trajectory, eq 20, in the q-space.

The resulting curves for different kh_0 corresponding to the cylinders depicted in Figure 2 are shown in Figure

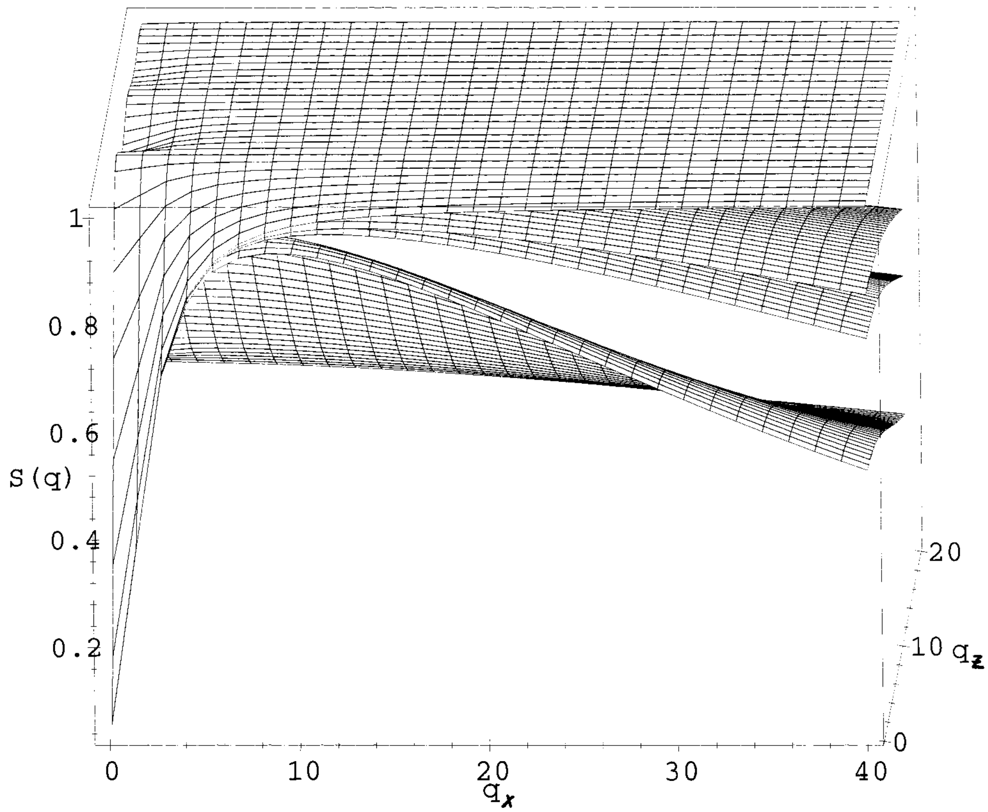

Figure 2. $S(\mathbf{q})$ for different values of the "gradient energy" parameter: $\beta = 0$, 6×10^{-5}, 10^{-4}, and 3×10^{-4} (from top to bottom).

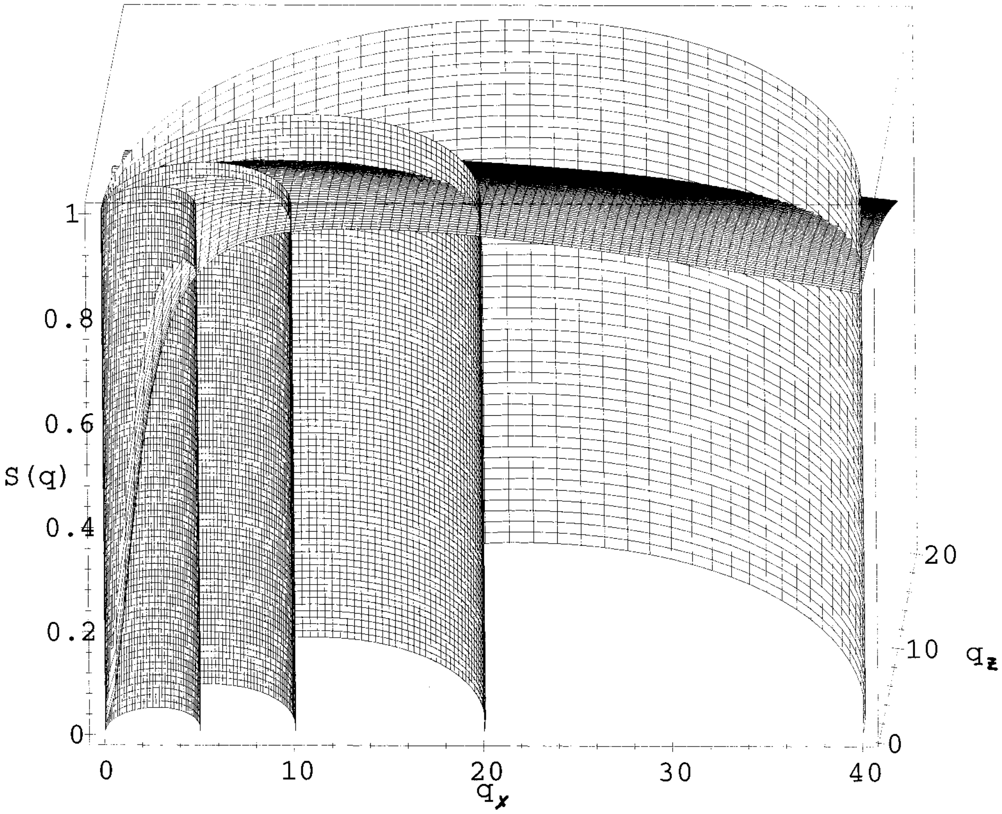

Figure 3. Scattering function $S(\mathbf{q})$ for a typical value, $\beta = 6 \times 10^{-5}$. The cylinders show the experimental $\mathbf{q}$-trajectories for kh_0 = 2.5, 5, 10, and 20 (from small to large).

4a. One can see that $S(\theta)$ is approximately constant for $\theta > 120°$ for $kh_0 \approx 2.5$ (this value of kh_0 was encountered in the experiments, see Table 1); a very weak maximum is predicted at large angles for $kh_0 > 2.5$. This maximum shifts to lower angles as kh_0 increases further. For $kh_0 \gtrsim 6$, the dependence of $S(\theta)$ shows a second maximum and a minimum. The position of the minimum tends to $\theta \approx 90°$ for large kh_0. The experimental data are shown in Figure 4b–d together with the theoretical plots for the values of kh_0 and β parameters listed in Table 1.

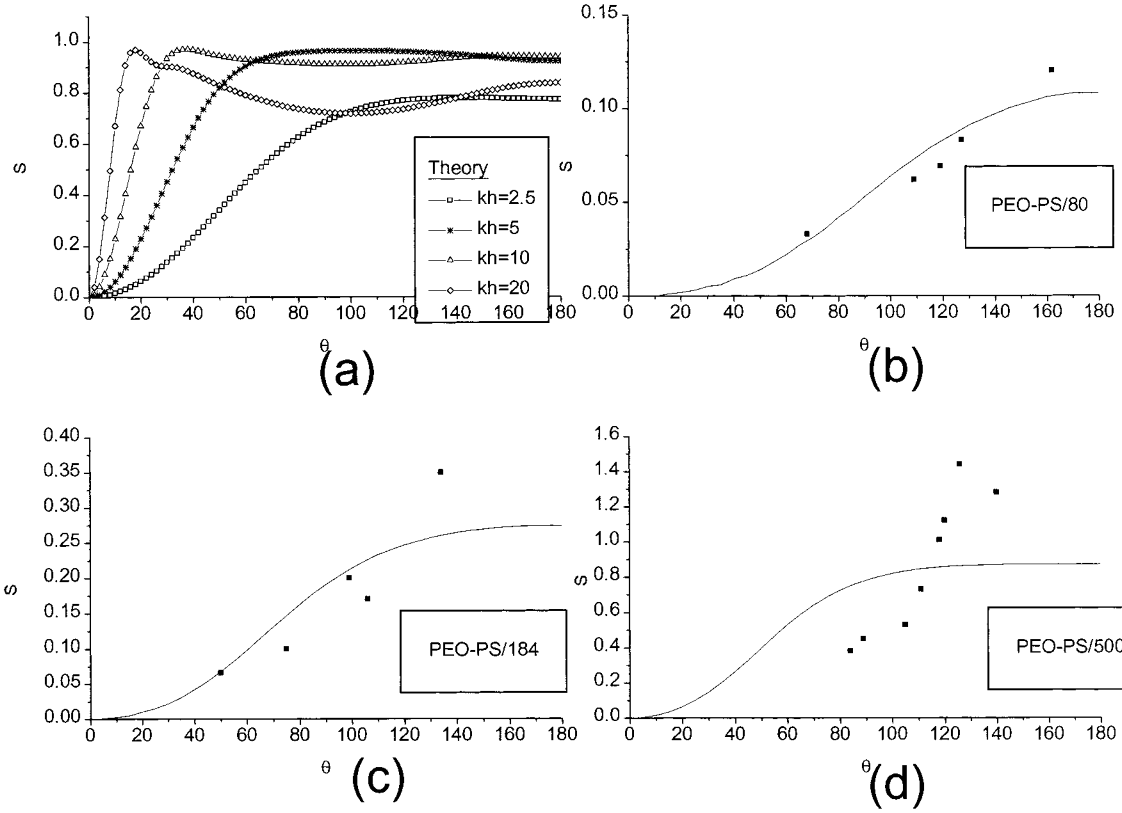

Figure 4. Scattering intensity as a function of the scattering angle, $S(\theta)$. (a) Theoretical predictions corresponding to the intersections between cylinders and surfaces in Figure 3. (b−d) Calculated and experimental scattering intensities for the three different brushes listed in the Table 1.

Table 1. Main Characteristics of Experimental Samples and the Values of kh_0 and β Parameters

sample	N	h_0 (nm)	σ (1/nm^2)	kh_0	β($\times 10^{-5}$)	Γ (mg m^{-2})
PEO−PS/80	730	45	0.020	0.87	9.8	2.9 ± 0.5
PEO−PS/184	1700	80	0.0083	1.5	6.4	2.6 ± 0.4
PEO−PS/500	4790	130	0.0019	2.5	5.8	1.7 ± 0.3

One can see that the agreement is rather good for short brushes, and it is poor for the longest brush. The main difference in the latter case is that the experimental $S(\mathbf{q})$ (see Figure 4d) increases first very slowly and than rapidly for large angles, whereas the theoretical scattering function is a quadratic function of q_x and q_z for small angles.

The limiting dependence of $S(q)$ for low wave vectors was also discussed in Fytas et al.[16] Using eqs 19 and 20 above, the low-q behavior of $S(q)$ (where $q = 2k_0 \sin \theta/2 \approx k_0\theta$) is predicted as

$$\lim_{\theta \to 0} S(q) = \frac{Lh_0}{12w}\frac{(qh_0)^2}{1 + 105\beta}$$

Here Lh_0 is the brush volume (per unit length in y-direction), which is proportional to the total adsorbed amount Γ. It is, therefore, predicted that the scattering intensity at low wave vectors is proportional to both the adsorbed amount and $(qh_0)^2$, which is in agreement with the experimental data.[16]

4. Concluding Remarks

The excess free energy of a small sinusoidal deformation of a "parabolic" polymer brush exposed to a marginal solvent is calculated in this paper. Two main contributions to the free energy, due to chain stretching and the inhomogeneous monomer distribution (the square-gradient term), are taken into account in the theory. The deformation energy is related to the scattering function defining the relative intensity of laser light scattered by the brush. We show that the scattering function depends on both components of the scattering wave vector: parallel to the grafting plane (q_x) and perpendicular (q_z). The scattering function attains a maximum at some q_m and it is small in the regimes of low and high q's. In the case $q_z = 0$ (scattering vector parallel to the brush) the maximum is controlled by the gradient term in the deformation energy, $q_m \sim 1/R$, where R is the unperturbed (Gaussian) size of grafted chains. However the evanescent-wave experimental setup implies that the scattering vector is tilted with respect to the grafting surface, so that q_z first increases and then decreases as q_x is increased. In this situation the scattering maximum is determined mainly by q_z variation rather than by the gradient energy, giving rise to a smaller $q_m \sim k \sim 1/h_0$ (where h_0 is the brush thickness and k is the wave vector of the incident beam).

The theoretical results have been compared with the scattering data first assuming that the evanescent-wave penetration depth, ξ_{ew}, is infinite.We have also calculated the scattering intensities for an arbitrary ξ_{ew}. The results show that the ξ_{ew}-effect is not important for the experimentally relevant values of $\xi_{\mathrm{ew}} \approx 0.4 \div 1$ μm.

The calculated dependencies of the scattering intensity on the scattering angle are in qualitative agreement with experimental data for all brushes except the thickest one. On the other hand, the disagreement between the theory and the data for the thickest brush is considerable, and we believe that it cannot be accounted for by lifting the model assumptions of marginal solvent conditions and of a monodisperse brush (in fact, the degree of polydispersity of grafted chains is not large, $M_w/M_n \approx 1.1$). It is possible that this discrepancy is due to the fact that the experimentally measured intensity does not correspond to the total static scattering, but rather, it includes contributions from a finite frequency range. It is possible that for the thickest brush one of the relaxation processes shifts outside this range so that it is no longer captured at low q's. However, at present, we do not have any evidence as to the origin of this process, so that the nature of the discrepancy remains an open issue.

Acknowledgment. We acknowledge that part of this research was sponsored by NATO's Scientific Affairs Division in the framework of the Science for Stability Programme and by the Greek General Secretariat of Research and Technology.

References and Notes

(1) Milner, S. T. *Science* **1991**, *251*, 905.
(2) Milner, S. T.; Witten, T. A.; Cates, M. E. *Macromolecules* **1988**, *21*, 2610.
(3) Fredrickson, G. H.; Ajdari, A.; Leibler, L.; Carton, J. P. *Macromolecules* **1992**, *25*, 2882−2889.
(4) Alexander, S. *J. Phys. (Paris)* **1977**, *38*, 983.
(5) Xi, H. W.; Milner, S. T. *Macromolecules* **1996**, *29*, 4772−4776.
(6) Grosberg A. Yu.; Khokhlov, A. R. *Statistical Physics of Macromolecules*; American Institute of Physics: New York, 1994.
(7) Semenov, A. N. *Sov. Phys. JETP (Engl. Transl.)* **1985**, *61*, 733.
(8) Landau, L. D.; Lifshitz, E. M. *Statistical Physics*; Pergamon Press: Oxford, 1998.
(9) Note that we consider two-dimensional ($x-z$) system here: the brush is always uniform in the y-direction.
(10) DeGennes, P. G. *Scaling Concepts in Polymer Physics*; Cornell Univ. Press: Ithaca, NY, 1985.
(11) Note that the interpenetration layer thickness ξ is different from the evanescent-wave penetration depth, ξ_{ew}.
(12) Semenov, A. N. *Macromolecules* **1993**, *26*, 2273.
(13) Semenov, A. N. *Macromolecules* **1992**, *25*, 4967.
(14) Broseta, D.; Fredrickson, G. H.; Helfand, E.; Leibler, L. *Macromolecules* **1990**, *23*, 122.
(15) Witten, T. A.; Leibler, L.; Pincus, P. *Macromolecules* **1990**, *23*, 824.
(16) Fytas, G.; Anastasiadis, S. H.; Seghrouchni, R.; Vlassopoulos, D.; Li, J.; Factor, B. J.; Theobald, W.; Toprakcioglu, C. *Science* **1997**, *274*, 2041.

MA980572S